

Clinical Ultrasound of the Salivary Glands

Philippe Katz, MD^{a,*}, Dana M. Hartl, MD, PhD^b, Agnès Guerre, MD^a

KEYWORDS

• Sialitis • Ultrasound • Color Doppler • Sialolithiasis • Tumors

Since the 1980s, ultrasound (US) has been shown to be a highly sensitive means of evaluating the major salivary glands. Because of technological advances and the superficial location of the major salivary glands, most regions are now accessible by high-resolution transducers. Only a small portion of the deep lobe of the parotid gland may be hidden by the acoustic shadow of the mandible.¹ Linear transducers with high frequencies between 7.5 and 16 MHz are used. In large lesions, transducers with a lower frequency may be used to completely visualize the lesion.

Salivary gland US should always be performed on both sides; many lesions occur bilaterally. If a tumor is suspected, the cervical lymph nodes should be examined as well. Color Doppler may be useful to investigate inflammatory lesions and tumors. Color Doppler is performed by comparing the vessel density with a normal reference gland or by comparing the vessel density of the tumor with the normal parenchyma. The peak systolic flow is generally measured, but the correction for the angle of the Doppler beam may be difficult to calculate in some cases. In Sjogren's syndrome, for example, the systolic peak velocity after salivary stimulation (with lemon juice) is often double the peak velocity in the resting state.

ULTRASONOGRAPHIC ANATOMY

All salivary glands are homogeneous echogenic organs. The normal sizes of the salivary glands have been evaluated.² The parotid gland measures on average 46 mm in its vertical dimension and 37 mm in its horizontal dimension, with a thickness of 7 mm anteriorly and 22 mm posteriorly. The submandibular gland measures approximately 33 × 35 × 14 mm. There does not seem to be any gender-related differences, but the size of the glands increases significantly with body weight.²

^a Salivary Glands Functional Explorations Institut, 7, Rue Theodore de Banville, 75017 Paris, France

^b Department of Otolaryngology Head & Neck Surgery, Institut Gustave Roussy, 39 rue Camille Desmoulins, 94805 Villejuif Cedex, France

* Corresponding author.

E-mail address: drkatz.philippe@gmail.com (P. Katz).

Parotid Gland

The parotid gland is located in the retromandibular fossa. Anatomically, the superficial lobe and deep lobe are separated by the plane of the facial nerve. On US, the nerve cannot be visualized and thus the anatomic lobes cannot be distinguished. Some refer to the caudal portion of the parotid gland as the superficial lobe, but we prefer referring to structures visualized around or within the gland for orientation, which avoids confusion with the anatomic definition of the parotid lobes. In most cases, the retromandibular vein is visualized without difficulty; however, normal intraglandular salivary ducts and the main duct (Stensen's duct) are generally not seen, even with high-frequency transducers. A dilated Stensen's duct may be visualized, running superficially along the masseter muscle through the corpus adiposum buccae and then turning medially through the buccinator muscle. In this anterior region, accessory salivary tissue can often be seen. The echostructure is usually homogeneous and the echogenicity comparable to that of the thyroid gland. Lymph nodes can be seen within the gland, and are located in the anatomic superficial lobe.

On US, the parapharyngeal space is only rarely visualized with sufficient quality. The internal carotid artery, the internal jugular vein and the posterior belly of the digastric muscle are not always seen. Because of acoustic absorption and dispersion, the deep part of the parotid gland is often difficult to visualize (**Fig. 1**).

Submandibular Gland

The submandibular gland is located anterior and caudal to the parotid gland. Sometimes the salivary tissues of both glands can be found adjacent to each other without any intervening fascia, but their echostructure is different: the submandibular gland is more hypoechoic than the parotid gland. The other anatomic structures in the submandibular region are the mandible, the mylohyoid muscle, the anterior belly of the digastric muscle, and the facial vessels.³ The facial artery runs posterior to or even within the submandibular gland. On a typical oblique section of the submandibular gland, the palatine tonsil can also be visualized as hypoechoic area in a cranio-posterior position relative to the submandibular gland. Normally, the submandibular glands have a triangular shape with a posterior base. Normal intraglandular ducts are only rarely visualized. After stimulation with lemon, they may be more easily



Fig. 1. Longitudinal sonogram of a normal parotid gland. 1: parenchyma, 2: small duct, 3: retromandibular vein, 4 and 5: external carotid artery.

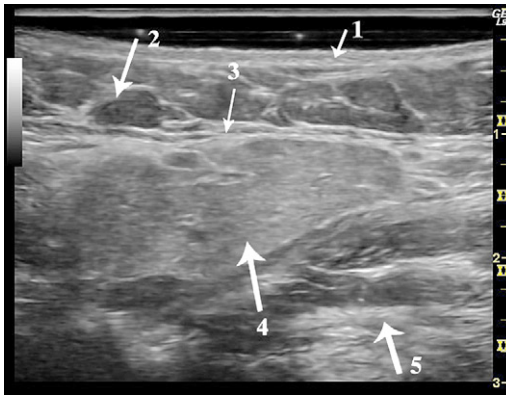


Fig. 2. Transverse sonogram of right normal submandibular gland. 1: skin, 2: fat, 3: fascia, 4: parenchyma, 5: mylohyoid muscle.

seen. The main submandibular duct (Wharton's duct) originates from the deep portion of the gland and ascends anteriorly to the caruncula in the floor of the mouth. The main duct can be differentiated from the lingual vessels by color Doppler (**Fig. 2**).

Sublingual Gland

The sublingual glands are localized in the floor of the mouth, cranial to the mylohyoid muscle, medial to the mandible and lateral to the geniohyoid muscle. In some cases the salivary tissue can even extend posteriorly to the submandibular gland.⁴ The sublingual glands have multiple small excretory ducts that are not visible with US. The glands appear more echogenic than the hypoechoic muscles of the floor of the mouth (**Fig. 3**).

SALIVARY GLAND INFECTIONS OR SIALITIS

Infection of a salivary gland is called *sialitis*, which can be further divided into infection of the gland itself, or *sialadenitis*, and infection of the salivary duct or ducts, termed *sialodochitis*. This section will cover the most common infections.



Fig. 3. Transverse sonogram of right normal sublingual gland. 1: parenchyma, 2: anterior belly digastric muscle, 3: floor of the mouth.

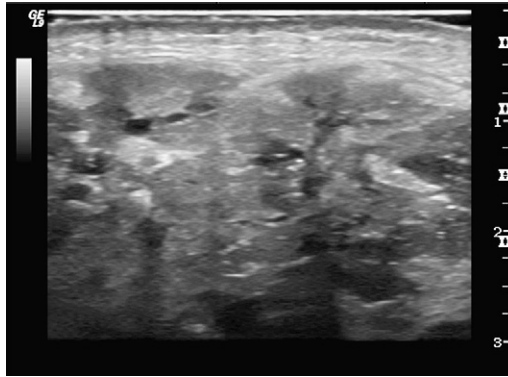


Fig. 4. Longitudinal ultrasound of a parotid gland. Unilateral heteroechogenic aspect of the parenchyma with duct dilatation and swelling of the gland.

Viral Sialadenitis

Endemic parotitis or the mumps, caused by a paramyxovirus, is the most frequent acute infection, even in the era of systematic vaccination. Usually, the clinical presentation is sufficient for a definitive diagnosis.⁵ In 75% of cases both parotid glands are enlarged. Cervical lymph nodes are also always enlarged. On US, the parotid glands are enlarged with a more rounded shape, a convex lateral surface, and a hypoechoic structure.^{6,7} Sometimes the salivary ducts are enlarged and visible. Color Doppler demonstrates diffuse hypervascularization.

Bacterial Sialadenitis

Acute bacterial parotitis

Normally the saliva within the salivary glands is sterile. Bacterial infection can originate in several ways. The most common origin is retrograde infection via the oral cavity, bacteria infecting the gland by way of the salivary duct. Less common origins include extracapsular spread of temporomandibular joint infections and hematogenous septicemia.

Acute bacterial parotitis is as common in adults as in children. Clinical presentation is typically unilateral, with sudden pain and swelling and increased pain at each meal (salivary colic, even in the absence of lithiasis). The examination of the ostium reveals

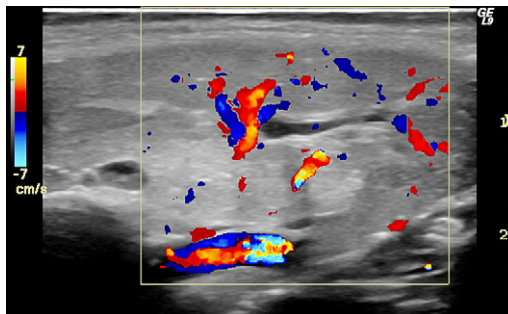


Fig. 5. Longitudinal ultrasound of parotid gland. Color Doppler reveals hyperemia. Acute sialoadenitis.

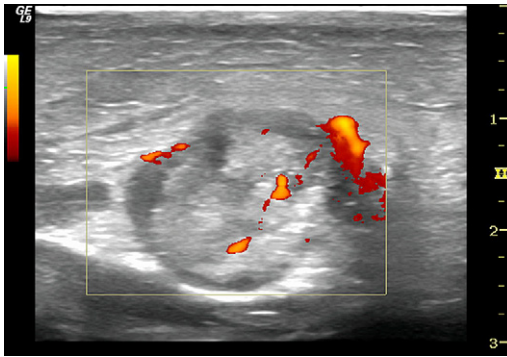


Fig. 6. Transverse sonogram and Doppler of a left parotid. Typical aspects of parotid abscess.

cloudy saliva or pus. Sialadenitis in adults is associated in approximately 50% of cases with sialolithiasis.

US is the only radiographic examination indicated, revealing salivary duct dilations, hypoechoic parenchyma, and enlarged intraglandular lymph nodes (**Fig. 4**). Hypervascularization because of the inflammation is visible on color Doppler (**Fig. 5**). The main goal of US in inflammatory diseases is to rule out lithiasis or other ductal obstructions.^{8,9} In severe infections, intraglandular liquid spaces, implying abscess formation, may be observed and are more frequent in diabetic patients. Air may also be seen,¹⁰ as well as moving, echogenic debris within an abscess.¹¹ US guidance is particularly useful for needle aspiration or drainage of the abscess (**Fig. 6**).

Acute bacterial submandibulitis

Acute bacterial submandibulitis occurs suddenly, with submandibular pain and swelling. Pus and debris may be seen at the Wharton's duct ostium in the floor of the mouth. US is essential for diagnosis (**Fig. 7**). The gland is heterogeneous with dilatation of the salivary ducts and increased vascularization on Doppler (**Fig. 8**). US is also necessary in this case to rule out an associated lithiasis.

Pediatric chronic bacterial parotitis

Chronic bacterial parotitis in children is a relatively common disease. Occurring at age 2 or 3, more rarely at a younger age, this sialadenitis presents initially like an acute viral

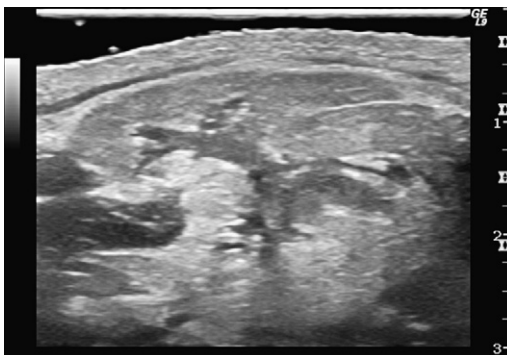


Fig. 7. Transverse ultrasound of left submandibular gland. Hypoechoic parenchyma and ducts dilatation. Acute submandibularis.

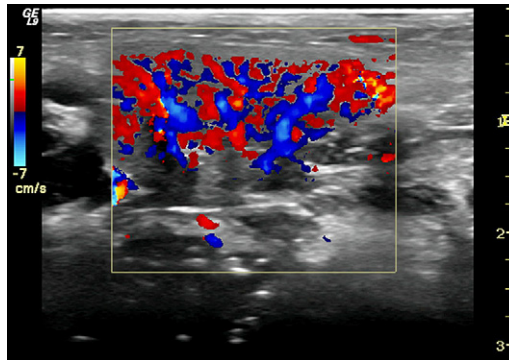


Fig. 8. Transverse color Doppler of left submandibular gland with hyperemia, acute submandibularis.

infection. Then it evolves unilaterally or bilaterally with episodes of acute pain and swelling and enlarged cervical lymph nodes.

US is indicated as soon as the first symptoms occur. Images are typical and pathognomonic.^{12–14} Multiple hypoechoic, cystoid areas and 2- to 3-mm vacuoles in the parotid glands are caused by the destruction of the glandular tissue by the chronic infection, and can take on a milary aspect on US (**Figs. 9** and **10**). Focal destruction of the glandular tissue can also cause salivary duct ectasia, which can be visualized on US. Small hyperechoic calcifications, which are not lithiases but a reaction to the inflammation, may also be seen. The Doppler shows hypervascularization of the gland and of the intra- and extraglandular lymph nodes (**Fig. 11**).

Chronic parotitis in adults

In chronic inflammation, the glandular modifications seen on US are often less prominent than in acute diseases. An atrophic hypoechoic gland may be seen, but the size of the gland is variable. Sometimes ductal ectasia is found (**Fig. 12**); however, sialography is superior to US for visualizing chronic inflammatory obstructions of the salivary ducts.

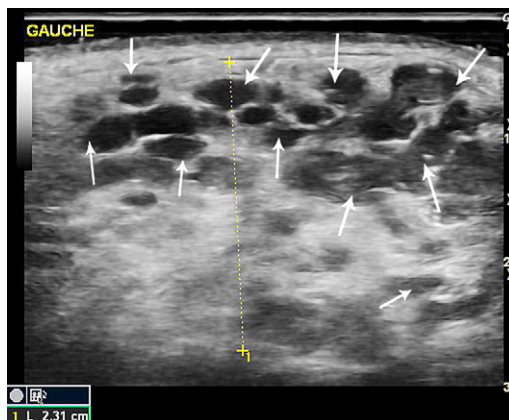


Fig. 9. Longitudinal sonogram of left parotid in a 6-year-old boy. Heteroechoic structure with many hypoechoic nodules (*arrows*). Typical aspects of chronic parotitis.

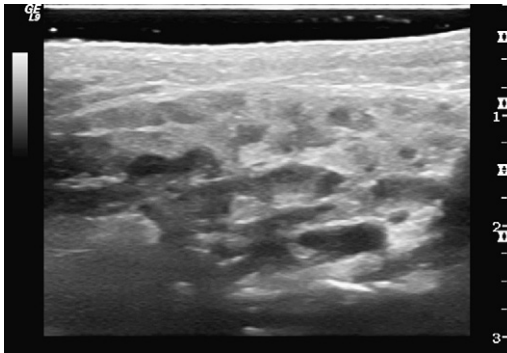


Fig. 10. Longitudinal sonogram of right parotid on an 8-year-old girl. Heteroechogenic structure with moderate hypoechoic nodules. Moderate chronic parotitis.

Adult chronic parotitis may occur in a patient having suffered from chronic or acute parotitis as a child or with a history of acute parotitis, or in the context of a systemic disease such as Sjogren's syndrome. It can also be secondary to a stricture or stenosis of a salivary duct, itself secondary to an acute infection.

US shows partial destruction of the gland, which is heterogeneous with hypoechoic regions representing destroyed parenchyma and hyperechoic regions of sclerosis. Dilatation of the salivary ducts with strictures or stenosis is always found, with strictures along Stensen's canal creating a "string of pearls" image. Ductal ectasia may also be present. Lymph nodes are visible within the gland and in the cervical regions. Doppler may or may not show hypervascularization, according to whether inflammation is present or not.

Tuberculous parotitis

Tuberculosis of the salivary glands is rare, with parotitis mimicking a malignant tumor. Moderate pain, or no pain at all, may be present. On US, there are heterogeneous, hypoechoic, poorly-defined lesions, with regional lymphadenopathy (**Fig. 13**). The lymph nodes themselves have poorly defined margins as well (**Fig. 14**).¹⁵ US-guided fine-needle aspiration (FNA) cytology is diagnostic showing specific granulomatous lesions with giant cells and necrosis.

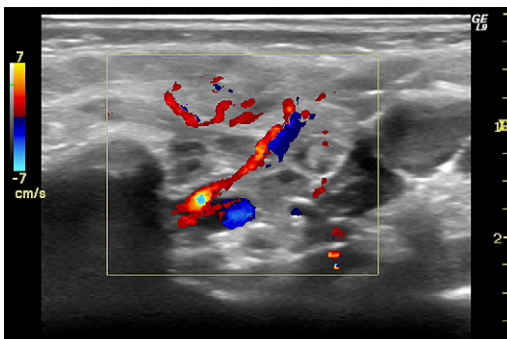


Fig. 11. Transverse color Doppler of left parotid gland in a 5-year-old girl. Moderate hyperemia with two big hypoechoic lymph nodes posteriorly.

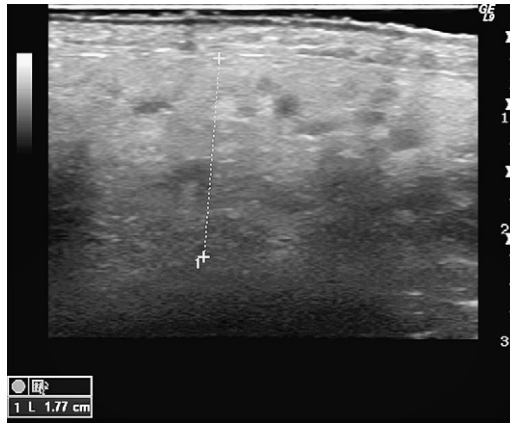


Fig. 12. Longitudinal sonogram of left parotid on an adult. Heteroechoic structure with small hypoechoic nodules. Chronic parotiditis.

Idiopathic Dilatation of the Salivary Ducts

This problem is attributable to a stricture or stenosis located at the level of the sphincter of the main salivary duct that causes a dehiscence of the wall of the duct. The dilatation resembles a hernia of the main salivary duct, occurring during meals. As the disease progresses, pain can also occur, giving rise to a salivary colic, and bilateralization generally occurs. At this stage, the duct can be seen and palpated under the skin of the cheek.¹⁵ It occurs most often in Stensen's duct of the parotid gland, primarily in females.

US confirms the diagnosis, showing a major dilatation of the duct with a diameter of up to 1 cm, all along the duct (**Fig. 15**). The stenosis is generally well visualized, and may be located anywhere along the canal (**Fig. 16**). No lithiasis is visible (**Figs. 17** and **18**). The glandular tissue may be hypotrophic with other dilated ducts. Signs of infection are often associated with the disease because of the stagnation of saliva within the gland. Doppler shows hypervascularization along the wall of the duct and also at the level of the stenosis.

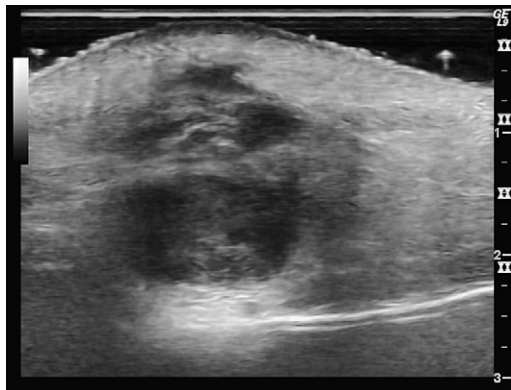


Fig. 13. Longitudinal sonogram of parotid on an adult. Big lesion inside the parenchyma badly delimitate with heteroechoic aspect mimic a tumor: tuberculosis.

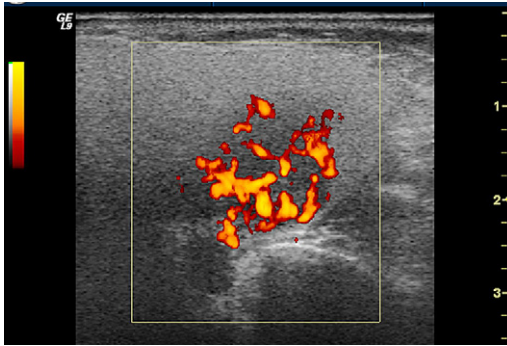


Fig. 14. Color Doppler of parotid tuberculosis. Hyperemia inside the lymph nod.

Sialodochitis with Sialolithiasis

It is now generally acknowledged that lithiasis formation can be found during early childhood, around the age of 1 year, but even earlier in some cases (our youngest case was a 2-month-old girl). A genetic predisposition has also been shown, with more than 300 families identified. In our experience of 3500 cases of lithiasis over a 20-year period, we have observed that only one type of major salivary gland is involved per patient, uni- or bilaterally; we have never observed lithiasis in different types of glands (parotid and submandibular, for example) in the same patient. Submandibular and parotid lithiasis show the same composition, but with different proportions of calcium and phosphate.¹⁵

More than 80% of salivary concretions are localized in the submandibular gland or in Wharton's duct. Approximately 15% of cases of sialolithiasis occur in the parotid gland or in Stensen's duct.¹⁶ Sublingual lithiasis is rare.¹⁷

Salivary calculi usually cause symptoms only if an obstruction of the ductal system occurs.¹⁸ For therapeutic purposes it is important to differentiate lithiasis of the main duct from those of the intraglandular ducts.¹⁹ Typical locations for lithiasis are at the anterior bend of Wharton's duct and at the confluence of the intraglandular ducts. Sometimes intraoral transducers are used to localize submandibular stones.²⁰ Lithiasis of the parotid system is often located in the ducts in the periphery of the gland or deep in the parenchyma.

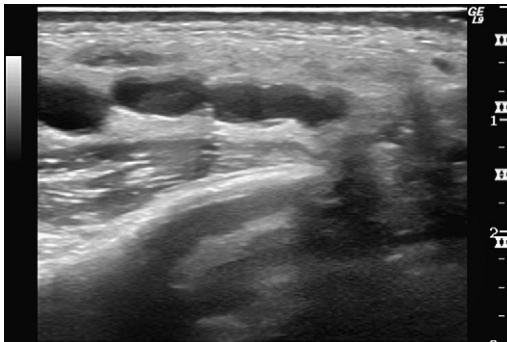


Fig. 15. Transverse sonogram of left parotid. Excretory duct dilatation with stenosis.

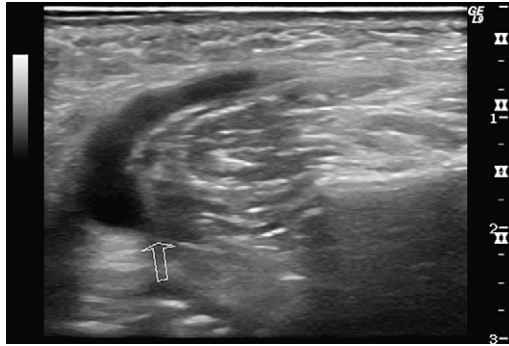


Fig. 16. Transverse sonogram of a left parotid. Stenosis on Stensen's duct (arrow).

Sonographically, lithiasis typically appears as a bright curvilinear echo complex with posterior shadowing (Figs. 19 and 20).²¹ In lesions smaller than 2 mm, this shadow may be missing (Fig. 21).

In symptomatic sialolithiasis, a concomitant dilatation of the ductal system or inflammation is often visualized (Fig. 22). Intraglandular duct ectasia presents as multiple tubular hypoechoic structures, whereas the dilated main duct is located in an extraglandular position and has a more linear shape. Inflammatory changes render the gland diffusely hypoechoic and with more rounded, globular margins. Color Doppler shows hypervascularization.

The accuracy of US in the assessment of sialolithiasis is approximately 90%.²² It is possible to differentiate calcified lymph nodes and phleboliths in facial veins from sialolithiasis. Approximately 20% to 40% of the salivary lithiasis are not opaque on plain films, but most of these stones are visible on US. Salivary stimulation (lemon or vitamin C) leads to more prominent intraglandular ducts. This facilitates the visualization of small lithiasis and the echogenic lithiasis contrast better with the dilated hypoechoic ducts.

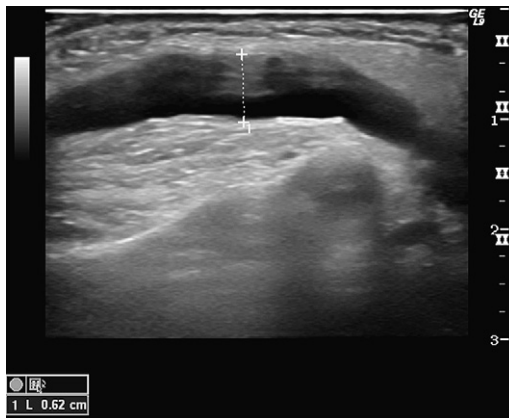


Fig. 17. Transverse sonogram of parotid. Important dilatation of the Stensen's duct.

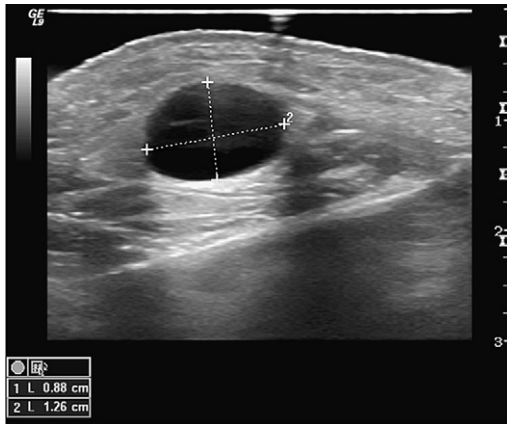


Fig. 18. Longitudinal sonogram of parotid gland. Wide dilatation of the duct.

In experienced hands, US is the primary method for detecting salivary calculi. Computed tomography, MRI,²³ or sialography can be reserved for those patients with inconclusive sonographic results or for patients with negative sonographic results and a typical clinical presentation of ductal obstruction.

Sialosis

The term of *sialosis* designates all the chronic diseases of the salivary glands that are not infections or tumors. This includes nutritional, dystrophic, and systemic diseases affecting the salivary glands. Most of these diseases are characterized by a hyperplasia of the salivary gland or glands, termed *sialomegaly*, and with deficit in salivary secretion.

Sialoadenosis

Often diabetes, alcoholism, and anorexia nervosa are clinically evident.²⁴ US shows enlarged glands with a hyperechoic structure and no focal lesions. Because of the



Fig. 19. Transverse ultrasound of right submandibular gland. Heteroechoic aspect of the gland with a white hyperechoic structure inside the pelvis. Sialolithiasis (6.7 mm diameter).

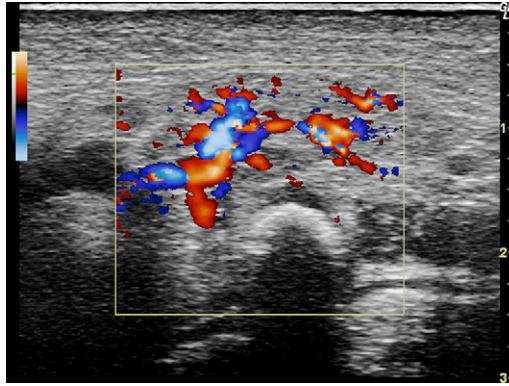


Fig. 20. Same gland as in Fig. 19 with color Doppler showing hyperemia.

high echogenicity, the deep portions of the parotid glands are usually not visualized (Fig. 23). Sometimes low-frequency transducers have to be applied to delineate the glands completely. Hypervascularization, as often found in acute inflammation, should be ruled out by demonstration of normal or subnormal color Doppler saturations (Fig. 24). In these bilateral painless enlargements of the glands it is important to rule out tumors and ductal obstructions. This can be performed by demonstration of a homogeneous glandular structure.

Systemic Sialosis

Sjogren's syndrome

Sjogren's syndrome (SS) is an autoimmune disease with chronic inflammation of the major salivary glands, the lacrimal glands, and arthritis. The exocrine glands are infiltrated by lymphocytes and plasma cells. The incidence of Sjogren's disease in women is seven to nine times higher than in men. Usually, patients present with a sicca complex. Often the antinuclear antibodies (ANAs) are positive, especially the subsets Anti-Ro/SSA, Anti-La/SSB. Definitive diagnosis is made by biopsy of the minor salivary glands of the lips.

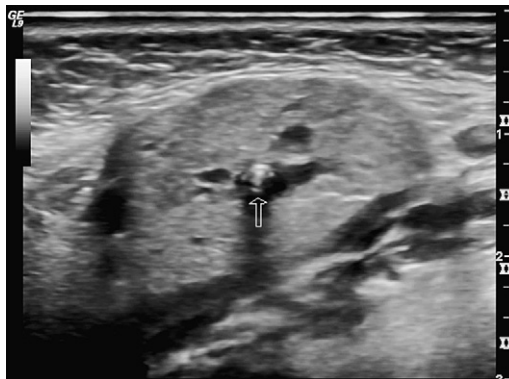


Fig. 21. Transverse ultrasound of right submandibular gland. Small lithiasis inside the pelvis less than 1 mm (arrow).

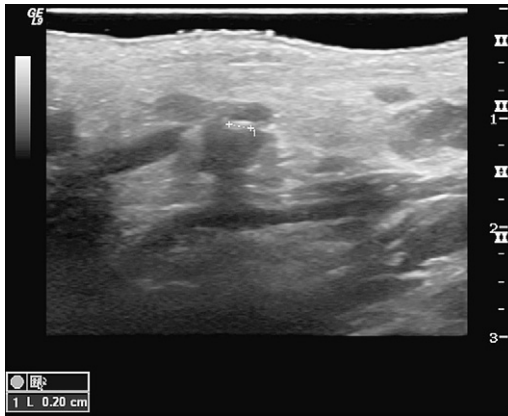


Fig. 22. Longitudinal sonogram of parotid gland. Hyperechogenic signal inside the pelvis with duct dilatation all around: sialolithiasis.

In SS, usually all of the major salivary glands are involved. In the acute stage, swelling and hypoechoic transformations are found.^{25,26} Often the glands are heterogeneous because of inflammation, enlarged lymph nodes, and myoepithelial hyperplasia (**Fig. 25**). The peripheral ductal system may be dilated; furthermore, multiple small cysts are found.²⁷ The sonographic changes correlate with histological involvement (**Fig. 26**).²⁶ With time, the glands become small, hypoechoic, heterogeneous, and difficult to delineate (**Fig. 27**).

Color Doppler shows hypervascularization in the acute inflammatory stage²⁸; however, when the salivary production is impaired owing to chronic fibrotic changes, the arterial blood flow reaction caused by stimulation is diminished.²⁹ Salivary stimulation causes a significant elevation of the arterial blood flow. In SS, the maximum systolic flow velocity is often doubled.³⁰

An important issue in SS is to rule out malignant lymphoma, which has an increased incidence in this disease; however, in a heterogeneous gland it is difficult to rule out small lesions through imaging. For hypoechoic lesions larger than 2 cm and for rapidly growing lesions, a biopsy should be performed.

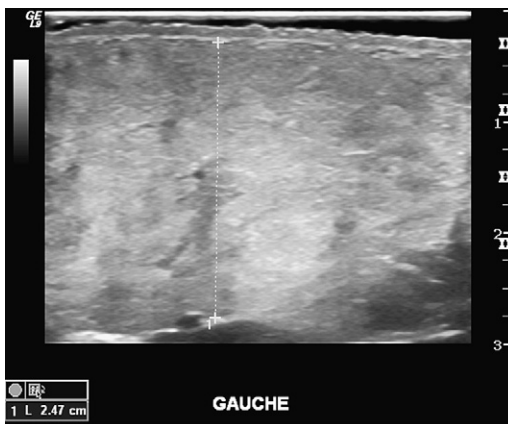


Fig. 23. Longitudinal sonogram of left parotid. Enlarged homogeneous gland, increased volume, lightly hyperechogenic. Anorexia syndrome.

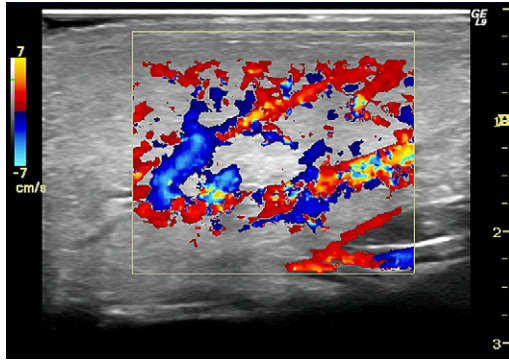


Fig. 24. Same gland as in Fig. 23 with the color Doppler showing hypervascularization and inflammation.

Kimura's disease

Kimura's disease, a non-neoplastic-hyperplastic multinodular lymph node disease, occurs predominately in the Asian population.³¹ Often the cervical lymph nodes and the nodes in the salivary glands are involved. No specific, distinguishable sonographic signs have been described, however.

SALIVARY GLAND TUMORS

Benign Tumors of the Glandular Epithelium

Pleomorphic adenoma

Pleomorphic adenoma is the most frequent tumor of the salivary tissue (24%–71%).^{15,32,33} In approximately 80% of cases the tumor is located in the superficial part of the parotid gland. In approximately 10% of cases the deep part of the parotid gland is involved. Rarely, the lesion protrudes into the parapharyngeal space (“iceberg” tumors). Histologically, the lesion is composed of epithelial, myoepithelial, and mesenchymal tissue.

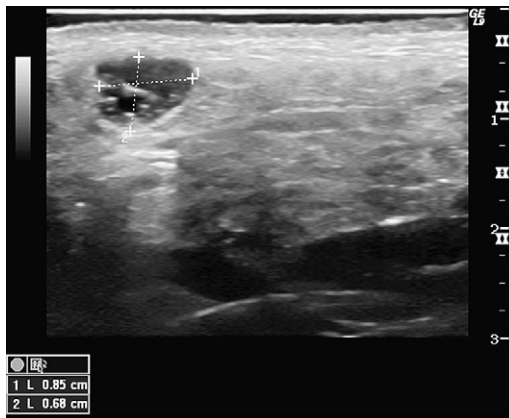


Fig. 25. Longitudinal sonogram of parotid gland. Heteroechoic structure like chronic parotitis with a big lymph node inside the parenchyma: Sjogren's syndrome.

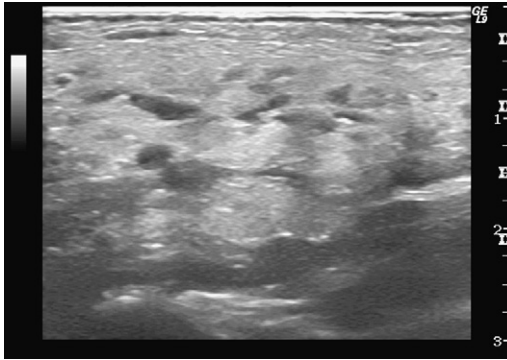


Fig. 26. Longitudinal sonogram of parotid gland. Lightly hyperechogenic structure of the parenchyma with ducts dilation hypoechoic: Sjogren's syndrome.

Sonographically, the tumor is well circumscribed and usually is homogeneous and hypoechoic. A well-defined, lobulated margin is regarded as typical (**Figs. 28 and 29**).³⁴ When calcifications are found in parotid tumors, pathology reveals a pleomorphic adenoma in most cases, although some malignancies also commonly show calcifications.³⁵ Color Doppler most often demonstrates moderate vascularization. A predominately peripheral flow pattern has been described.³⁶ Maximum systolic flow most often is below 25 cm/s (**Figs. 30 and 31**).³⁴ Pleomorphic adenoma of the submandibular gland occurs in approximately 10% of cases (**Figs. 32 and 33**).

Pleomorphic adenoma is usually a slowly growing lesion. Surgery is recommended. Malignant transformation has been reported in up to 5% of cases. Rapid growth of a formerly stable parotid mass is suspicious for carcinoma ex pleomorphic adenoma. Blurry, ill-defined borders are suspicious for malignancy.

Cystadenolymphoma (Warthin's tumor)

Papillary cystadenoma lymphosum (Warthin's tumor) is the second most frequent salivary gland tumor. On palpation these tumors are usually soft and compressible, unlike pleomorphic adenomas. The tumors are most often located in the caudal part of the parotid gland and may be bilateral. Cystadenolymphomas of the submandibular gland are rare.

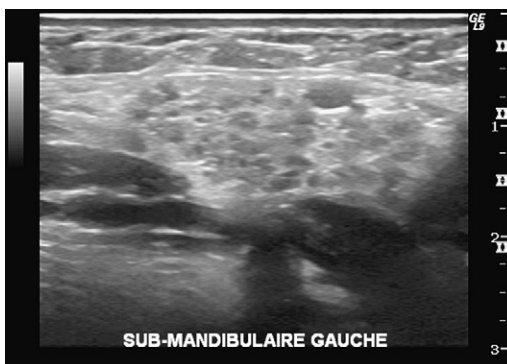


Fig. 27. Transverse ultrasound of left submandibular gland. Typical aspect of Sjogren's syndrome, with many hypoechoic nodules inside the parenchyma.

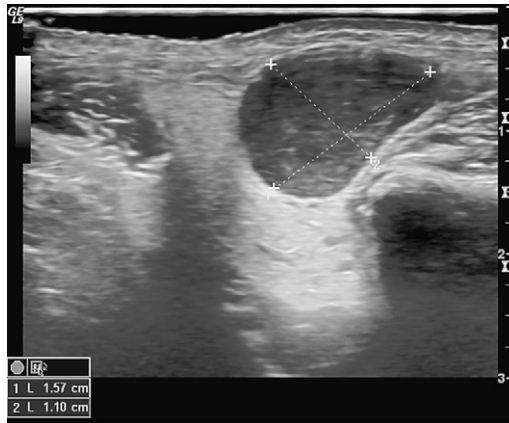


Fig. 28. Transverse sonogram of right parotid gland. Homogeneous hypoechoic tumor well delimitate inside the parenchyma. Histology demonstrated pleomorphic adenoma.

On pathology, the tumors are composed of epithelial and lymphatic tissue. Cystic parts within a solid lesion are regarded as typical for Warthin's tumor (**Figs. 34 and 35**).^{36–38} Often they present with an ovoid shape. On US the lesion is usually more heterogeneous than pleomorphic adenomas (**Fig. 36**).^{35,38} and have well-defined borders. These tumors are multicentric in up to 30% of cases.³⁶ Recurrent tumors are not unusual. Nuclear medicine studies after salivary stimulation show a higher uptake than the normal parenchyma; therefore, this tumor can be diagnosed relatively specifically. If large cystic lesions are present, however, the technetium scan may be negative.³⁹ Oncocytoma may also show a strong tracer uptake on scintigraphy and be mistaken for a cystadenolymphoma.

Malignant Epithelial Tumors

Mucoepidermoid carcinoma

Mucoepidermoid carcinoma is the most frequent malignant tumor of the salivary glands. These tumors are differentiated pathologically into two main groups:

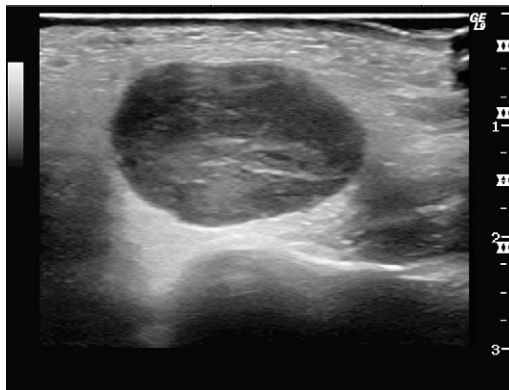


Fig. 29. Longitudinal sonogram of gland parotid gland. Aspect homogeneous hypoechoic of a tumor. Fine needle aspiration cytology (FNAC) diagnosed a pleomorphic adenoma.

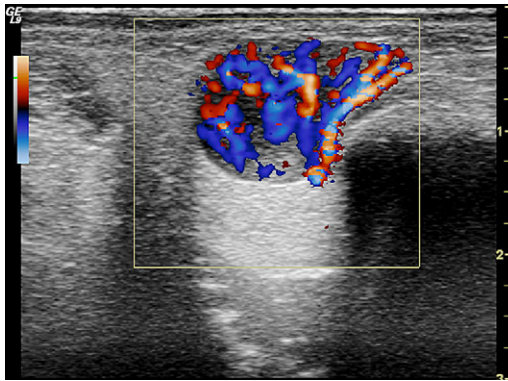


Fig. 30. Transverse sonogram of right parotid gland. Color Doppler inside a well-delineated hypoechoic tumor. Hypervascularization inside a pleomorphic adenoma.

carcinoma with a high grade of malignancy and tumors with a low grade of malignancy. Malignant tumors smaller than 2 cm in diameter usually have a homogeneous structure and present with smooth borders; therefore, especially low-grade malignant tumors are often incorrectly diagnosed as benign lesions by imaging.³² High-grade malignant tumors and larger lesions mostly show irregular borders and a typical heterogeneous echo pattern. Frequently, irregular zones of necrosis are found. These tumors are most often correctly assessed as malignant tumors by US.

In larger lesions, the main drawback of US is its incapacity to completely delineate the tumor. Infiltrations of the parapharyngeal space, the base of the skull, or the mandible are not accessed by US.

Adenoid cystic carcinoma

Adenoid cystic carcinoma is also sometimes misdiagnosed as a benign lesion (**Fig. 37**). The typical perineural infiltrations are usually not detected by US. Acinus cell carcinoma, squamous cell carcinoma, undifferentiated carcinoma, or adenocarcinoma are less frequent.

In malignant tumors, color Doppler usually shows a higher degree of vascularization as compared with the normal parenchyma or with benign tumors. High systolic values

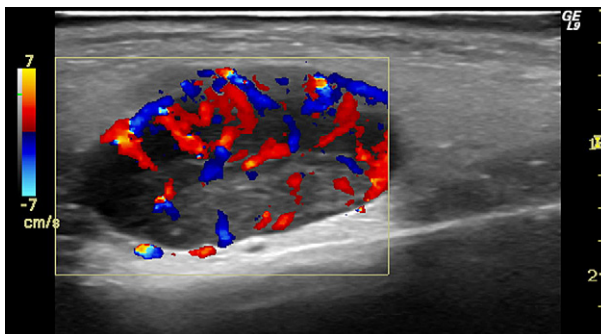


Fig. 31. Longitudinal sonogram of gland parotid gland. Color Doppler inside a well-delineated hypoechoic tumor. Hypervascularization inside a pleomorphic adenoma.



Fig. 32. Transverse ultrasound of right submandibular gland. Hypo to isoechogenic tumor inside the gland well delineated: pleomorphic adenoma.

and a chaotic pattern of tumor vessels are suspicious for malignancy, even when gray-scale imaging suggests a benign lesion³⁴; however, up to now, color Doppler of salivary gland tumors is a method under clinical investigation. No criteria are known to definitively differentiate between benign and malignant tumors.

Nonepithelial Tumors

Lymph node metastases within the parotid gland

Intraglandular lymph node metastases most often present as multiple, round, well-defined lesions (**Fig. 38**). Lymph node metastases of the parotid gland are most commonly caused by malignant melanoma, squamous cell carcinoma, or metastatic carcinoma of the lung or breast. Malignant lymphoma (non-Hodgkin's lymphoma) may also involve the salivary glands. Most often, multiple hypoechoic, well-defined lesions are present. Color Doppler usually shows hypervascularization.

Lipomas

Lipomas are rare salivary gland tumors. Both CT and MRI reveal a specific morphology by demonstration of fat-equivalent tissue; therefore, whenever a lipoma is suspected clinically or on US, one of these investigations should be performed.

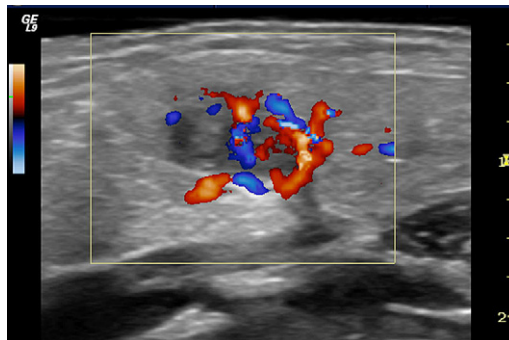


Fig. 33. Same gland with the color Doppler, see the hypervascularization inside the tumor.

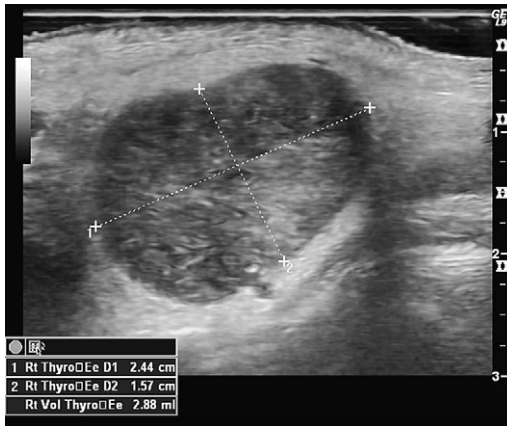


Fig. 34. Transverse sonogram of right parotid gland. Hypo to isoechogenic lesion with several cystic areas, but well delineated. FNAC reported papillary cystadenoma lymphosum or Whartin's tumor.

On US, these relatively soft, fat-containing tumors typically have an ovoid shape, sharp outlines, and are moderately compressible. Compared with the parotid parenchyma, pure fat-containing lipomas are moderately hypoechoic lesions.^{40–42} Typically, a striated, feathered echogenicity is found (**Fig. 39**). Fibrolipomas are only slightly hypoechoic with regard to the parotid tissue. Lipoblastomas usually reveal cystic components. On color Doppler, lipomas show no or very little Doppler signal.

Liposarcomas are rare tumors in the salivary gland region. The diagnosis should be considered in fast-growing echogenic tumors.

Neurogenic tumors

Neurogenic tumors (schwannomas, neurofibromas) in the cervical soft tissue present as spindle-shaped lesions with a connection to the originating nerve. However, the facial nerve is not visible in the parotid gland; therefore, the specific diagnosis is rarely established on US. Neurogenic tumors often present with cystic areas. Usually moderate vascularization is present in color Doppler. Malignant schwannomas have been described.

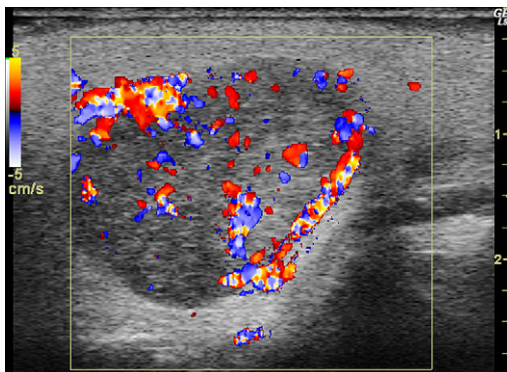


Fig. 35. Same tumor with color Doppler seeing lightly hyperemia.

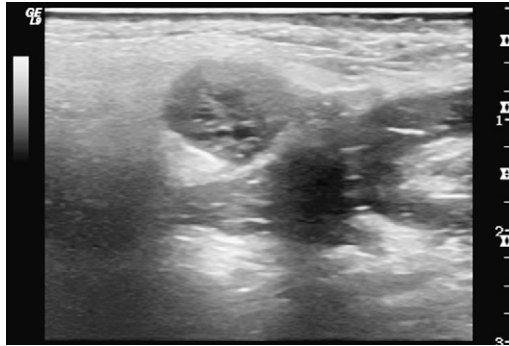


Fig. 36. Longitudinal sonogram of gland parotid gland. Hypo to isoechogenic lesion with several cystic areas but well delimitate. FNAC reported papillary cystadenoma lymphotosum.

Hemangiomas and lymphangiomas

In children, hemangiomas are the most frequent tumors of the salivary gland regions.⁴³ The diagnosis is usually made by clinical findings. Imaging is needed in deep-seated lesions, when the overlying skin is normal, or when the lesion encroaches on vital structures. On US, hemangiomas usually appear as hyperechoic, ill-defined lesions, or as hypoechoic lesions with a typical lobular pattern (**Figs. 40** and **41**).⁴⁴ Hemangiomas are compressible. Color Doppler shows hypervascularity, which is defined as more than five color structures per square centimeter. Pulsed Doppler shows a peak systolic flow of up to 90 cm/s. The diastolic flow is also increased with spectral broadening and a low resistive index (RI: 0.4–0.7).⁴³

In most cases, spontaneous involution occurs in adolescence; however, when significant complications, such as bleeding, compression of vital structures, or coagulopathy are present, they are treated surgically or by embolization. In these therapeutic cases, CT or MRI is indicated to delineate the lesion completely.

Approximately 75% of lymphangiomas occur in the neck. Usually they are located in the posterior compartment. Histologically, a combination of cystic hygroma, cavernous, capillary, and vascular-lymphatic malformations may be present within

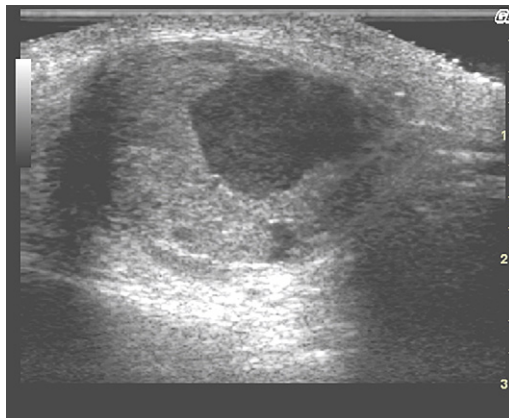


Fig. 37. Longitudinal sonogram of gland parotid gland. Heterogeneous tumor inside the parenchyma, with a hypoechoic cyst. Histology was adenoid cystic carcinoma.

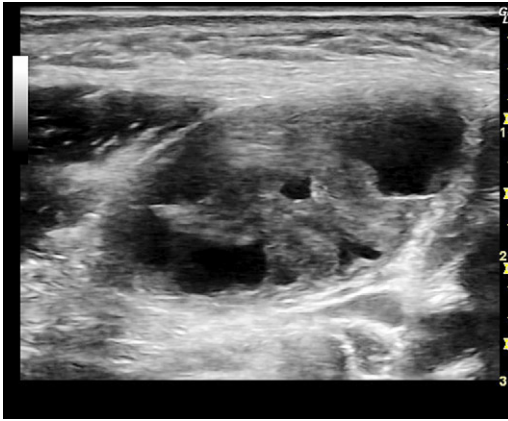


Fig. 38. Lymph node metastases to the salivary gland.

a single lesion. On US, they are predominantly cystic lesions with septae of variable thickness (**Fig. 42**). The echogenic components correspond to clusters of atypical lymphatic vessels, which are too small to be seen owing to the spatial resolution of US.⁴⁵ When hemorrhage or infection is present, the cysts contain floating debris. On color Doppler, lymphangioma appears avascular or hypovascularized (**Fig. 43**). Lymphangiomas are often surgically treated. In macrocystic lymphangioma, sclerosing therapy can be performed under US guidance.⁴⁶

Dermoid cysts

Occasionally dermoid tumors are found in the salivary gland region. Usually these dysontogenetic cysts are localized in the midline in the floor of the mouth. These tumors can be echogenic owing to the high acoustic impedance between fluid, fat, hair, and sebaceous material (**Fig. 44**).

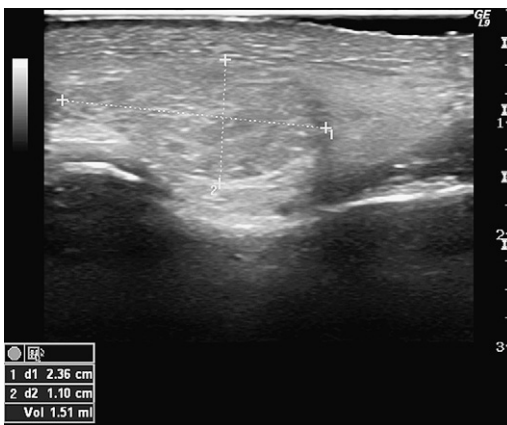


Fig. 39. Longitudinal sonogram of gland parotid gland. Moderately hypoechoic lesion with smooth borders. Notice the fine hyperechoic trabeculation inside the lesion, a typical aspect of lipoma.



Fig. 40. Transverse sonogram of right parotid gland of a 6-month-old baby. Big lobulated hypoechoic lesion inside the gland indicative of hemangioma.

Basal cell adenomas

Basal cell adenomas are rare. They generally involve minor salivary glands or accessory salivary tissue. Usually, a solid encapsulated lesion is found⁴⁷ (**Fig. 45**).

PSEUDOTUMORS

Masseter Muscle Hypertrophy

Unilateral hypertrophy of the masseter muscle is often misdiagnosed.⁴⁸ Hypertrophy of the masseter muscle can be assumed if the masseter measures more than 14 mm in its short-axis diameter at rest.

First Branchial Cleft Cysts

Cysts of the first branchial cleft, which are usually located in the parotid parenchyma, can be echogenic; they may mimic a solid tumor.⁴⁹ Most often these lesions are strictly homogeneous, and sometimes floating echoic cholesterol crystals may be

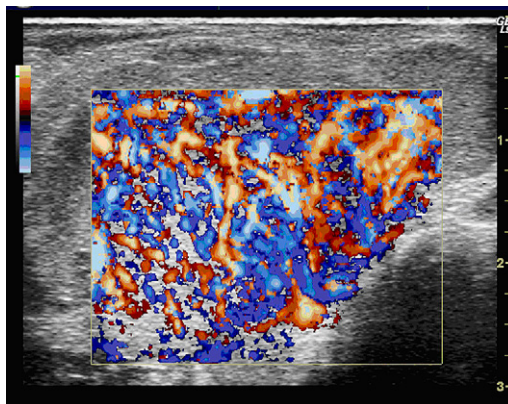


Fig. 41. Same patient as in Fig. 40 with the color Doppler: see the important hypervascularization inside the lesion.



Fig. 42. Transverse sonogram of right parotid gland. Very big hypoechoic lesion located at the bottom of the parotid gland with fine hyperechoic cluster typical of lymphangioma.



Fig. 43. Same patient as in Fig. 42 with color Doppler. See the hypovascularization of the lesion.

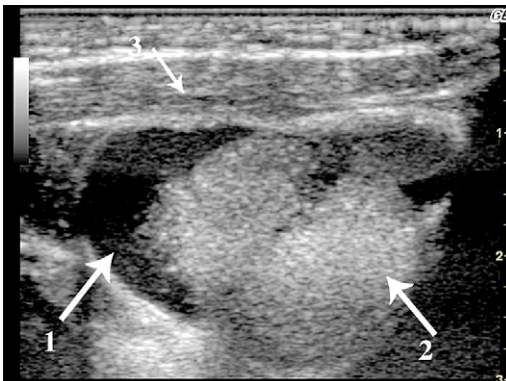


Fig. 44. Transverse sonogram of the floor of the mouth with a dermoid cyst. 1: hypoechoic part of the cyst, 2: hyperechoic part of the cyst, 3: anterior belly of digastric.

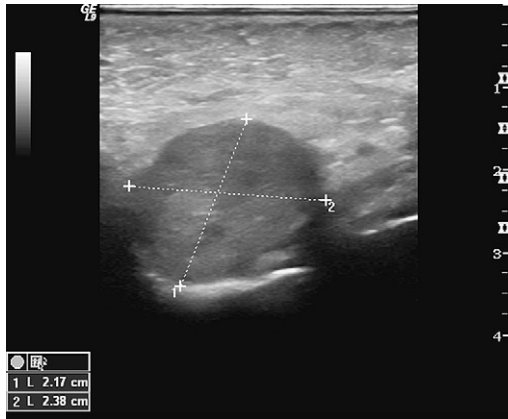


Fig. 45. Transverse sonogram of right cheek. Huge lesion at the internal face of the cheek, lightly hypoechoic, encapsulated. Cytology was a basal cell adenoma.

mobilized by palpation. Color Doppler should be used to evaluate the intrinsic vascularization.

Retention Cysts (Ranulae)

These benign lesions generally occur following trauma involving the floor of the mouth. These retention cysts (ranulae) of the sublingual gland can appear hypoechoic.⁵⁰ The cyst is always very well delineated in the floor of the mouth (**Figs. 46** and **47**).

Chronic Sclerosing Sialadenitis

Chronic sclerosing sialadenitis (Kuttner's tumor) generally involves the submandibular gland. These hypoechoic pseudotumors should be investigated carefully to visualize the ductal structures of the lesion, which are typical for Kuttner's tumor.

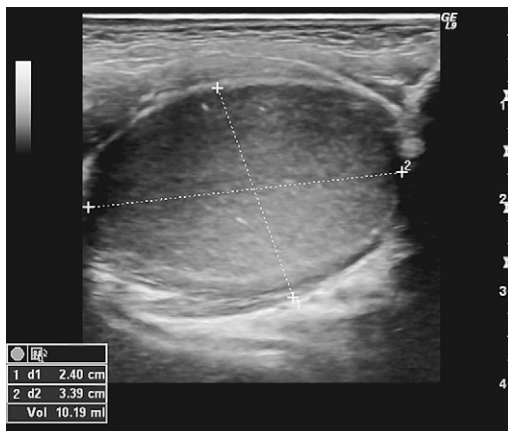


Fig. 46. Transverse sonogram of right floor of the mouth. Huge hypoechoic lesion very well delineated and encapsulated located under the Wharton's canal: a ranula.



Fig. 47. Clinical aspects of the ranulae.

AIDS-related Lymphoepithelial Cysts

Depending on the clinical presentation, a mixture of multiple cystic and solid lesions may be caused either by lymphoepithelial cysts in AIDS or by sarcoidosis. In benign lymphoepithelial lesions in AIDS, gray-scale US shows a broad range of findings. Usually the parotid glands are enlarged with multiple cystic or hypoechoic lesions, but mixed lesions and septae can also be detected. Color Doppler shows a variety of avascular or hypervascularized lesions.^{51–54} In most cases the cervical lymph nodes are enlarged. In these patients it is difficult to exclude malignant lymphoma by imaging.

SUMMARY

In most clinical situations, US is the first-line imaging method in the evaluation of the major salivary glands. In inflammation and infection, US differentiates obstructive and nonobstructive sialoadenitis. In sialolithiasis, US can differentiate intraductal from intraglandular lithiasis and visualize radiotransparent lithiasis. Concomitant obstruction and inflammation can be evaluated. In Sjogren's syndrome, US correlates with histological grade.

US is very sensitive in detecting tumors and lymph nodes. Superficial tumors can be delineated, whereas large or deeply located tumors usually require MRI. The specificity of US in differentiation of tumors is limited, but US is important for guiding FNA. Pseudotumors, such as tuberculosis, sarcoidosis, Kuttner's tumor, and intraglandular lymphadenopathy, should be distinguished from true neoplasms. With progress in ultrasound technology such as elastography, US distinction between benign and malignant tumors may be possible in the near future.

REFERENCES

1. Katz P. Nouvel apport de l'échographie en pathologie maxillo-faciale [Salivary glands, new approach by sonography]. *Inf Dent* 1990;72:2593–8.
2. Dost P, Kaiser S. Ultrasonographic biometry in salivary glands. *Ultrasound Med Biol* 1997;23:1299–303.
3. Gritzmann N, Fruhwald F. Sonographic anatomy of the tongue and floor of the mouth. *Dysphagia* 1988;2:196–202.

4. Yasumoto M, Nakagawa T, Shibuya H, et al. Ultrasonography of the sublingual space. *J Ultrasound Med* 1993;12:723–9.
5. Tarantino L, Giorgio A, de Stefano G, et al. Ultrasonography in the diagnosis of post-pubertal epidemic parotitis and its complications. *Radiol Med* 2000;99:461–4.
6. Schurawitzki H, Gritzmann N, Fezoulidis J, et al. Value and indications for high-resolution real-time sonography in nontumor salivary gland diseases. *Rofa* 1987;146:527–31.
7. Schwerk WB, Schroeder HG, Eichhorn T. High-resolution real-time sonography in salivary gland diseases. I. Inflammatory diseases. *HNO* 1985;33:505–10.
8. Ching AS, Ahuja AT, King AD, et al. Comparison of the sonographic features of acalculous and calculous submandibular sialadenitis. *J Clin Ultrasound* 2001; 29:332–8.
9. Kessler A, Strauss S, Eviatar E, et al. Ultrasonography of an infected parotid gland in an elderly patient: detection of sialolithiasis during the acute attack. *Ann Otol Rhinol Laryngol* 1995;104:736–7.
10. Curtin JJ, Ridley NT, Cumberworth VL, et al. Pneumoparotitis. *J Laryngol Otol* 1992;106:178–9.
11. Nusem-Horowitz S, Wolf M, Coret A, et al. Acute suppurative parotitis and parotid abscess in children. *Int J Pediatr Otorhinolaryngol* 1995;32:123–7.
12. Shimizu M, Ussmuller J, Donath K, et al. Sonographic analysis of recurrent parotitis in children: a comparative study with sialographic findings. *Oral Surg Oral Med Oral Pathol Oral Radiol Endod* 1998;86:660–5.
13. Nozaki H, Harasawa A, Hara H, et al. Ultrasonographic features of recurrent parotitis in childhood. *Pediatr Radiol* 1994;24:98–100.
14. Rubaltelli L, Sponga T, Candiani F, et al. Infantile recurrent sialectatic parotitis: the role of sonography and sialography in diagnosis and follow-up. *J Radiol [Br]* 1987;60:1211–4.
15. Katz P, Heran F. Pathologies des glandes salivaires [Salivary gland pathologies]. *Encyclopédie Médico-chirurgicale (Elsevier, Masson, SAS, Paris), radiodiagnostic cœur-poumon* 2007;32-800-A-30.
16. Gritzmann N, Hajek P, Karnel F, et al. Sonography in salivary calculi: indications and status. *Rofa* 1985;142:559–62.
17. Traxler M, Gritzmann N. Sonographic detection of salivary calculi of the sublingual gland. *Rontgenblätter* 1986;39:328–9.
18. Zenk J, Constantinidis J, Kydles S, et al. Clinical and diagnostic findings of sialolithiasis. *HNO* 1999;47:963–9.
19. Yoshimura Y, Inoue Y, Odagawa T. Sonographic examination of sialolithiasis. *J Oral Maxillofac Surg* 1989;47:907–12.
20. Brown JE, Escudier MP, Whites EJ, et al. Intra-oral ultrasound imaging of a submandibular duct calculus. *Dentomaxillofac Radiol* 1997;26:252–5.
21. Gritzmann N. Sonography of the salivary glands. *Am J Roentgenol* 1989;153:161–6.
22. Bartlett LJ, Pon M. High-resolution real-time ultrasonography of the submandibular salivary gland. *J Ultrasound Med* 1984;3:433–7.
23. Becker M, Marchal F, Becker CD, et al. Sialolithiasis and salivary ductal stenosis: diagnostic accuracy of MR sialography with a three-dimensional extended phase conjugate-symmetry rapid spinecho sequence. *Radiology* 2000;217:347–58.
24. Herrlinger P, Gundlach P. Hypertrophy of the salivary glands in bulimia. *HNO* 2001;49:557–9.
25. Ariji Y, Ohki M, Eguchi K, et al. Texture analysis of sonographic features of the parotid gland in Sjogren's syndrome. *Am J Roentgenol* 1996;166:935–41.

26. Salaffi F, Argalia G, Carotti M, et al. Salivary gland ultrasonography in the evaluation of primary Sjogren's syndrome. Comparison with minor salivary gland biopsy. *J Rheumatol* 2000;27:1229–36.
27. Bradus RJ, Hybarger P, Gooding GA. Parotid gland: US findings in Sjogren syndrome. Work in progress. *Radiology* 1988;169:749–51.
28. Steiner E, Graninger W, Hitzelhammer J, et al. Color-coded duplex sonography of the parotid gland in Sjogren's syndrome. *Rofo* 1994;160:294–8.
29. Chikui T, Yonetsu K, Izumi M, et al. Abnormal blood flow to the submandibular glands of patients with Sjogren's syndrome: doppler waveform analysis. *J Rheumatol* 2000;127:1222–8.
30. Arijii Y, Yuasa H, Arijii E. High frequency color Doppler sonography of the submandibular gland: relationship between salivary secretion and blood flow. *Oral Surg Oral Med Oral Pathol Oral Radiol Endod* 1998;86:476–81.
31. Ahuja AT, Loke TK, Mok CO, et al. Ultrasound of Kimura's disease. *Clin Radiol* 1995;50:170–3.
32. Koischwitz D, Gritzmann N. Ultrasound of the neck. *Radiol Clin North Am* 2000;38:1029–45.
33. Hausegger KW, Krasa H, Pelzmann W, et al. Sonography of the salivary glands. *Ultraschall Med* 1993;14:68–74.
34. Schick S, Steiner E, Gahleitner A, et al. Differentiation of benign and malignant tumors of the parotid gland: value of pulsed Doppler and color Doppler sonography. *Eur Radiol* 1998;8:1462–7.
35. Shimizu M, Ussmuller J, Hartwein J, et al. A comparative study of sonographic and histopathologic findings of tumorous lesions in the parotid gland. *Oral Surg Oral Med Oral Pathol Oral Radiol Endod* 1999;88:723–37.
36. Gritzmann N, Turk R, Wittich G, et al. Hochoauflosende sonographie nach operation von cystadenolymphomen der glandula parotis. *Rofo* 1996;145:648–51 [in German].
37. Klein K, Turk R, Gritzmann N, et al. The value of sonography in salivary gland tumors. *HNO* 1989;37:71–5.
38. Yoshiura K, Miwa K, Yuasa K, et al. Ultrasonographic texture characterization of salivary and neck masses using two-dimensional gray-scale clustering. *Dentomaxillofac Radio* 1997;26:332–6.
39. Miyake H, Matsumoto A, Hori Y, et al. Warthin's tumor of the parotid gland on Tc-99 m pertechnetate scintigraphy with lemon juice stimulation. Tc-99m uptake, size, and pathologic correlation. *Eur Radiol* 2001;12:2472–8.
40. Gritzmann N, Schratler M, Traxler M, et al. Sonography and computed tomography in deep cervical lipomas and lipomatosis of the neck. *J Ultrasound Med* 1988;7:451–60.
41. Gritzmann N. The diagnosis of salivary gland lipoma. *Rofo* 1989;151:419–22.
42. Chikui T, Yonetsu K, Yoshiura K, et al. Imaging findings of lipomas in the orofacial region with CT, US, and MRI. *Oral Surg Oral Med Oral Pathol Oral Radiol Endod* 1997;84:88–95.
43. Toma P, Rossi UG. Pediatric ultrasound. II. Other applications. *Eur Radiol* 2001;11:2369–98.
44. Yang WT, Ahuja A, Metreweli C. Sonographic features of head and neck hemangiomas and vascular malformations: review of 23 patients. *J Ultrasound Med* 1997;16:39–44.
45. Sheth S, Nussbaum AR, Hutchins GM, et al. Cystic hygromas in children: sonographic-pathologic correlation. *Radiology* 1987;162:821–4.
46. Dubois J, Garel L, Abela A, et al. Lymphangiomas in children: percutaneous sclerotherapy with an alcoholic solution of zein. *Radiology* 1997;204:651–5.

47. Raffaelli C, Amoretti N, Parlotti B. Salivary glands. In: Bruneton JN, editor. Applications of sonography in head and neck pathology. Berlin/Heidelberg/New York: Springer; 2002. p. 91–136.
48. Traxler M, Ertl U, Ulm C, et al. Sonographic diagnosis of the unilateral benign hypertrophic masseter muscle. *Z Stomatol* 1991;88:23–6.
49. Calderazzi A, Falaschi F, Esposito S, et al. First branchial arch cysts. A diagnostic assessment. *Radiol Med* 1989;77:420–2.
50. Horiguchi H, Kakuta S, Nagumo M. Bilateral plunging ranula. A case report. *Int J Oral Maxillofac Surg* 1995;24:174–5.
51. Mandel L. Ultrasound findings in HIV-positive patients with parotid gland swellings. *J Oral Maxillofac Surg* 2001;59:283–6.
52. Martinoli C, Pretolesi F, Del Bono V, et al. Benign lymphoepithelial parotid lesions in HIV-positive patients: spectrum of findings at gray-scale and Doppler sonography. *Am J Roentgenol* 1995;165:975–9.
53. Goddart D, Francois A, Ninane J, et al. Parotid gland abnormality found in children seropositive for the human immunodeficiency virus (HIV). *Pediatr Radiol* 1990;20:355–7.
54. Gritzmann N, Rettenbacher T, Hollerweger A, et al. Sonography of the salivary glands. *Eur Radiol* 2003;13:964–75.